Journal of Structural Geology 93 (2016) 149–161

Contents lists available at ScienceDirect

Journal of Structural Geology

journal homepage: www.elsevier.com/locate/jsg

An extension of the Saltykov method to quantify 3D grain size distributions in mylonites

Marco A. Lopez-Sanchez*, Sergio Llana-Fúnez

Departamento de Geología, Universidad de Oviedo, 33005, Oviedo, Spain

ARTICLE INFO

Article history:
Received 11 May 2016
Received in revised form
15 October 2016
Accepted 26 October 2016
Available online 27 October 2016

Keywords:
Grain size distributions
Saltykov method
Two-step method
Dynamic recrystallization
Mylonites
Lognormal distributions

ABSTRACT

The estimation of 3D grain size distributions (GSDs) in mylonites is key to understanding the rheological properties of crystalline aggregates and to constraining dynamic recrystallization models. This paper investigates whether a common stereological method, the Saltykov method, is appropriate for the study of GSDs in mylonites. In addition, we present a new stereological method, named the two-step method, which estimates a lognormal probability density function describing the 3D GSD. Both methods are tested for reproducibility and accuracy using natural and synthetic data sets. The main conclusion is that both methods are accurate and simple enough to be systematically used in recrystallized aggregates with near-equant grains. The Saltykov method is particularly suitable for estimating the volume percentage of particular grain-size fractions with an absolute uncertainty of ±5 in the estimates. The two-step method is suitable for quantifying the shape of the actual 3D GSD in recrystallized rocks using a single value, the multiplicative standard deviation (MSD) parameter, and providing a precision in the estimate typically better than 5%. The novel method provides a MSD value in recrystallized quartz that differs from previous estimates based on apparent 2D GSDs, highlighting the inconvenience of using apparent GSDs for such tasks.

1. Introduction

Grain size distributions (GSDs) in deformed crystalline aggregates reflect the conditions and processes during deformation and therefore are an important parameter to measure in mylonites. For example, they are key to constraining dynamic recrystallization (DRX) models. The current technical limitations for investigating three-dimensional phenomena imply that we cannot directly observe DRX processes in 3D during deformation. Hence, our complete understanding of DRX processes depends partly on numerical models (e.g. Derby and Ashby, 1987; Shimizu, 1998, 1999). A way to validate these DRX models is to compare whether the GSDs produced by them are similar to those observed in rocks deformed in nature or experimentally.

The rheological properties of crystalline aggregates depend partly on the GSDs. For example, GSDs have been used successfully to gain insights into the rock behaviour during deformation by tracking volume changes from transient to steady-state in the different grain-size fractions (Heilbronner and Bruhn, 1998; Ter Heege et al., 2002). Some authors also claim that calibration of flow laws are best achieved using GSDs instead of unidimensional values of grain size (e.g. De Bresser et al., 1998, 2001; Ter Heege et al., 2004; Herwegh et al., 2005; Shimizu, 2008). However, no generally accepted model exist yet concerning this matter and the current hypotheses require further study, including investigating the relations between GSDs and deformation behaviours.

Despite GSDs utility, estimating GSDs in crystalline aggregates is challenging, and their use is rare in rock deformation studies dealing with mylonites. Common methods for measuring directly 3D microstructures, such as serial sectioning or X-ray-based tomography (XRT), have serious limitations when attempting to characterize GSDs. Serial sectioning is very time-consuming, mostly suited for relatively small volumes, and challenging to apply in monomineralic aggregates with fine grain sizes (although see Rowenhorst et al., 2010 for an example in alloys). XRT does not distinguish touching crystals of the same phase, which is problematic when dealing with monomineralic mylonites. A very promising technique is the phase-contrast tomography (PCT) that can identify individual grain locations based on lattice-preferred orientation, allowing us to obtain the GSD (e.g. McDonald et al.,

* Corresponding author.
E-mail addresses: malopez@geol.uniovi.es (M.A. Lopez-Sanchez), slf@geol.uniovi.es (S. Llana-Fúnez).

http://dx.doi.org/10.1016/j.jsg.2016.10.008
0191-8141/

2015). However, because of its recent development, limited availability, and high cost, PCT studies are not yet common and, consequently, has not yet been used in mylonites. This state of affairs means that in practice we rely on the measurement of the apparent GSDs from 2D sections to derive 3D GSDs via stereological methods.

The most used stereological method in mylonites is the so-called Saltykov method (e.g. Heilbronner and Bruhn, 1998). The method depends on the assumption that neighbouring grains did not interact in the rock (i.e. the grains are isolated, in a similar to garnet porphyroblasts in a schist), but this assumption is never met in crystalline aggregates. Thus, a key question is whether the grain packing observed in mylonites invalidates the use of the method. Heilbronner and Barret (2014) claimed that by assuming random grain packing, a fair assumption in mylonites, and measuring a large number of grains the condition holds. This is because when a large number of grains is measured, we increased the chance of measuring a representative grain size population diluting the nearest neighbour local effect. Yet, the question of what is the minimum sample size needed to avoid this effect has not been validated analytically or empirically and, therefore, a previous test is required when using grain size maps from samples with random grain packing.

Another major limitation of the Saltykov method is that it lacks a complete quantitative description of the actual GSD. For example, the shape of the GSD cannot be quantified directly from the output obtained from the Saltykov method because the use of the histogram in the illustration of the grain size distribution only provides a qualitative view. We therefore see a need to find a method that overcomes this limitation.

The aims of this study are: i) to validate the use of the Saltykov method in the grain boundary maps with random grain packing; ii) to test the reliability of the Saltykov method in estimating the percentage of volume of a particular grain fraction; and iii) to find a reliable method for estimating a complete quantitative description of the actual 3D GSD.

2. Brief review of stereological methods for deriving actual 3D GSDs from thin sections

Stereology is a body of mathematical methods relating two-dimensional measurements to parameters defining a three-dimensional structure, which in the present case is the 3D GSD. For grain size studies, the stereological methods have to deal with the cut-section and the intersection probability effects (Fig. 1). The cut-section effect refers to the intersection plane rarely cutting exactly through the centre of each grain, so that measured grain profiles and sizes are mostly apparent rather than actual values. The intersection probability effect refers to larger grains being more likely than smaller grains to be represented on a section plane since their greater size gives them a greater probability of being hit by a section plane.

It is well known that actual 3D GSD can only be estimated from observations in a single section assuming spatial homogeneity between particles and for specific shape assumptions for the particles (Exner, 1972; Cruz-Orive, 1983; Higgins, 2006). These assumptions are that all particles are of the same shape and, for the analytical solution to the problem, that all particles are spherical (Wicksell, 1925). These geometrical assumptions and the unavoidable introduction of errors during grain boundary identification (e.g., over and under-segmentation, the optical and the image resolution limitation) severely restrict the practical relevance of all stereological methods. Furthermore, for other common (ideal) particle shapes in rock grains, such as ellipsoids or parallelepipeds, only rough solutions can be obtained as long as all the particles have the same shape and the overall grain shape ratios are known (e.g. Sahagian and Proussevitch, 1998; Higgins, 2000). Consequently, any stereological method for estimating 3D GSDs is biased and, at best, we only obtain acceptable approximations (Cruz-Orive, 1983; Chiu et al., 2013). A key condition for obtaining reliable GSD estimates via stereological methods is therefore to verify that grains have near-equant shapes. This assumption is acceptable most of the time for some of the most common dynamically recrystallized non-tabular grains in crustal and mantle shear zones, such as quartz, feldspar, olivine or calcite (e.g. Casey et al., 1998; Snoke et al., 1999; Mancktelow and Pennacchioni, 2004; Stipp and Kunze, 2008; Linckens et al., 2014), except when highly amoeboid grain shapes are present.

2.1. The Saltykov method: advantages and limitations

Although several stereological methods are available for deriving 3D GSDs from single sections (see review in Chiu et al., 2013), the most widely used method in the field of igneous and metamorphic petrology, is the so-called Scheil-Schwartz-Saltykov method (Scheil, 1931; Schwartz, 1934; Saltykov, 1967), usually shortened as the Saltykov method (e.g. Heilbronner and Bruhn, 1998; Sahagian and Proussevitch, 1998; Higgins, 2000). This method uses a histogram of grain size abundances and a sequential subtraction procedure to convert the distribution of apparent grain sizes into the actual 3D GSD (see Appendix A for details). The method is distribution-free, meaning that no assumption is made about the type of statistical distribution for the grain size population. The benefits of the Saltykov method are three-fold: First, it is versatile and sophisticated enough to deal with real data. In fact, the use of the histogram allows the method to better handle the unavoidable introduction of errors during grain segmentation, as well as to deal with grains that depart slightly from equant shapes (e.g. Sahagian and Proussevitch, 1998; Higgins, 2000). Second, it is free from distribution assumptions, which is crucial when dealing with multimodal distributions, common in mylonites. Third, it is simple and explicit enough to be implemented and used routinely by non-expert stereologists.

The Saltykov method has also some specific drawbacks. Due to the use of the histogram, the class sizes determines the accuracy and success of the method. However, a trade-off exists because the smaller the class size, the better the approximation of the targeted distribution, whereas the larger the class size, the better the numerical stability of the method. The issue with this trade-off is that no method exists to find an optimal class size or number of classes, so practitioners apply rules of thumb based on practical experience (Saltykov, 1967; Underwood, 1970; Exner, 1972; Sahagian and Proussevitch, 1998; Higgins, 2000). As a result, different authors select different number of classes based on their experience and subjective assessment.

Another limitation of the method is that it ignores the over-projection effect (Holmes, 1927; see also Cruz-Orive, 1983) (Fig. 1c), which can be a problem for crystalline aggregates in transmitted light microscopy containing a significant number of grains having diameters less than the thickness of the host thin section (usually of 30 μm). The problem can be avoided using ultrathin sections or techniques that obtain micrographs by interacting with the very first microns (or less) of the surface of the section, such as SEM-BSE or high-resolution SEM-EBSD maps.

The most important limitation of the Saltykov method is that due to the use of the histogram we cannot obtain a complete description of the GSD but rather only a qualitative view of the actual GSD, greatly limiting its utility for constraining dynamic recrystallization models. Some studies (e.g. Heilbronner and Bruhn, 1998) have derived the mean and the standard deviation from the

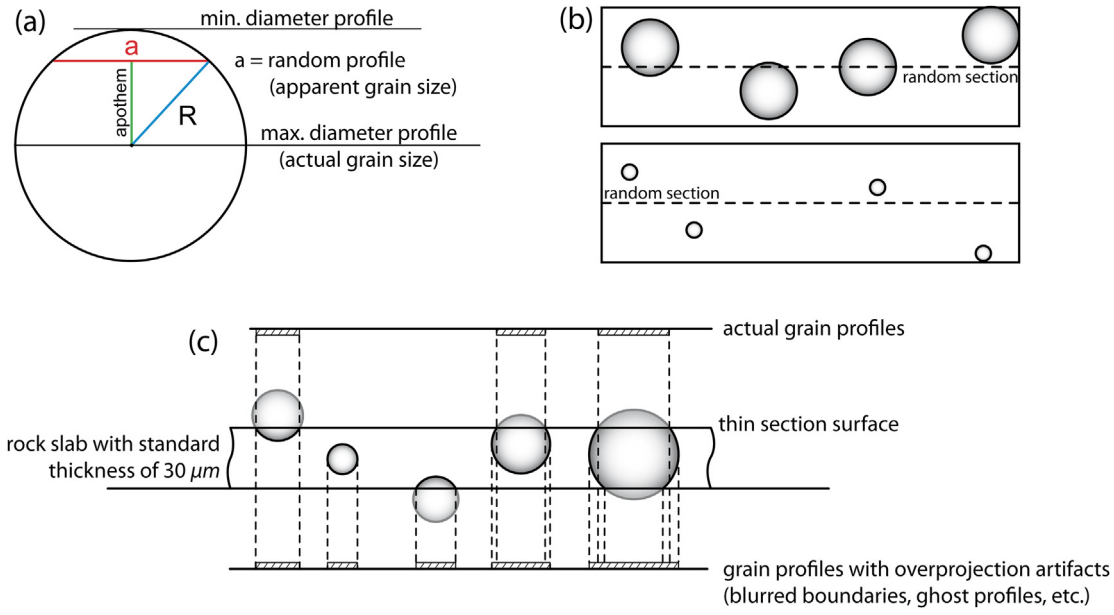

Fig. 1. Effects due to the use of thin sections through three-dimensional grains. (a) The cut-section effect. (b) The intersection probability effect. Both boxes contain the same number of particles. The probability of cutting such particles depend not only in their number but also in their size, because larger grains are more likely to intersect the section plane. (c) Overprojection effects in thin sections when using transmitted light microscopy.

Saltykov output, but this outcome requires making some assumptions, such as assuming that the grain sizes within each class are uniformly distributed. Moreover, when using a single data set it is impossible to obtain an uncertainty value during the estimation, since the Saltykov method do not return an error in the estimates of the frequencies of the different classes (e.g. Heilbronner and Barret, 2014). A way to overcome this limitation is to implement a parametric (distribution-based) method by assuming that the GSDs fits a well-known distribution (e.g. Gaussian, lognormal, etc.), since these methods are able to fully quantify the distribution of grain sizes using two or three parameters. To adopt this approach, it is essential to know which distribution best describes the grain size populations in dynamically recrystallized mylonites.

3. Grain size distributions in dynamically recrystallized rocks

The notion that mylonites invariably exhibit a specific GSD is well-known (e.g. Ranalli, 1984). However, the knowledge of the type and parameters that define the GSDs in mylonites remains elusive due to the absence of studies performing a direct measure of the GSD. Most authors working with naturally and experimentally recrystallized rocks realized that when using a logarithmic scale for the axis representing the apparent grain sizes of a particular mineral phase, the distributions resemble a Gaussian distribution (Michibayashi and Masuda, 1993; Newman, 1994; Dijkstra et al., 2002; Ter Heege et al., 2002, 2004; Slotemaker, 2006; see also Exner, 1972; Humphreys and Hatherly, 2004; for examples in alloys and references there in). This outcome was interpreted to indicate that dynamically recrystallized grains approach a lognormal distribution of grain sizes. This assessment has a limited validity since it is based on a characteristic of the apparent 2D GSD not the actual 3D GSDs. In the absence of direct GSD measures, a better approach is to look at the actual 3D GSDs derived using stereological methods. Using this approach, some authors found that completely dynamically recrystallized rocks show unimodal 3D GSDs skewed to the right at their linear scale or Gaussian-like using a logarithmic scale, approaching lognormal distributions even better than the apparent 2D GSDs (e.g. Heilbronner and Bruhn, 1998; Berger et al., 2011; Lopez-Sanchez and Llana-Fúnez, 2015). Thus, despite the approach being qualitative, it is reasonable to assume a lognormal distribution in completely recrystallized rocks.

3.1. Basic properties of lognormal distributions

A random variable x —in our case x is the size of the grain— is lognormally distributed if $\log(x)$ is normally distributed (Fig. 2) (Limpert et al., 2001). Lognormal distributions have two features, only positive values are possible and the distribution skews to the right on a linear scale (Fig. 2). The probability density function is often expressed as:

$$f(x/\mu,\sigma) = \frac{1}{x\sigma\sqrt{2\pi}} e^{\frac{-(\ln x-\mu)^2}{2\sigma^2}} \quad (1)$$

where μ and σ are the mean and the standard deviation of the function $\log(x)$, respectively. In this case, we consider the natural logarithms of the diameters of the grains. An alternative terminology, promoted by Limpert et al. (2001) and partially followed in this study, is to use the parameters scale (denoted as μ^*) and shape (denoted as σ^* or s^*), since they describe the data directly at their linear scale. As shown in Fig. 2, they correspond with the "back-transformed" values of mean (μ) and standard deviation (σ) of the $\log(x)$ distribution, and they are referred as the scale (μ^*) and the shape or multiplicative standard deviation (MSD) (s^*), respectively (Limpert et al., 2001). In a perfect lognormal distribution, the arithmetic mean and the frequency peak of the logarithmic grain-size population coincides with the geometric mean or median at the linear scale (Fig. 2). The relations between the different parameters in both terminologies are presented in Table 1. As the term shape is widely used in microtectonics to refer to the grain shape, hereafter we will refer to this parameter as the MSD parameter, instead. In a similar fashion, the term median will be used instead of the scale.

Fig. 3 shows that the MSD (s^*) controls the shape of the lognormal distribution. Thus, if s^* has a value of one, we obtain a

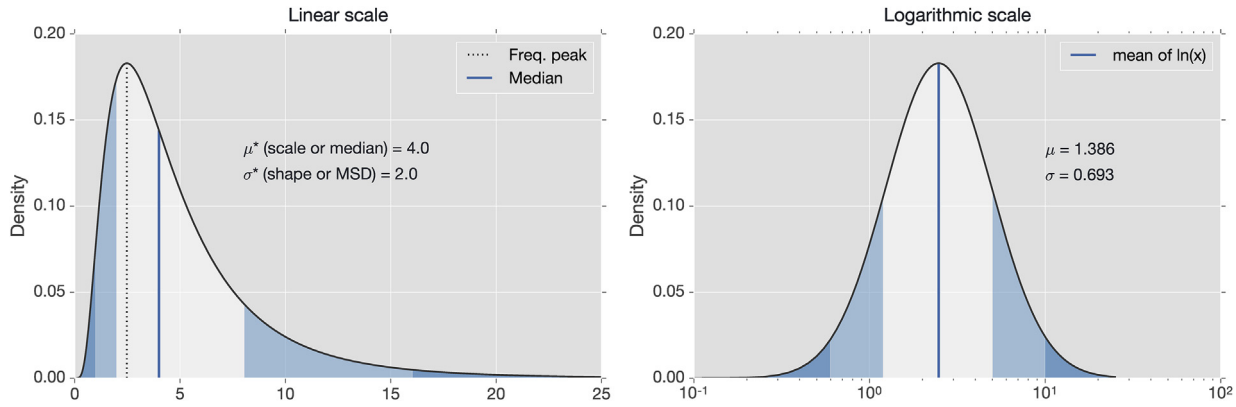

Fig. 2. A lognormal distribution with linear (left) and logarithmic scale (right). Areas under the curve correspond to one and two standard deviations of the log(x). Based on Limpert et al. (2001).

Table 1
Relations between different parameters at linear and logarithmic scales.

Linear scale		Logarithmic scale log(x)	
μ^* (scale or median)	e^{μ}	μ (mean)	log(median)[a]
s^* (shape or MSD)	e^{σ}	σ (std. Dev.)	log(shape)
freq. peak	$e^{\wedge}(\mu - \sigma\wedge 2)$	freq. peak	log(median)[a]
mean(x)	$e^{\wedge}(\mu - \sigma\wedge 2/2)$		

[a] The mean coincides with the freq. peak (mode) and the median in the logarithmic scale.

normal (Gaussian) distribution. However, if MSD has much larger values, the shape of the lognormal distributions becomes increasingly skewed to the right (Fig. 3a). On the other hand, the median (μ^*) parameter affects the scaling in horizontal (i.e. the range of the grain size) and vertical directions, but the shape remains the same (Fig. 3b). The lognormal probability density functions in Fig. 3a and b assume that the fixed bound to the left is set to zero. A shift parameter, usually referred as location, can be included in the function when data cannot be smaller than a certain bound different from zero (Yuan, 1933). However, a pilot study showed us that the difference in the estimates using the two- and the three-parameter approach are minor and that in some cases the location function provided negative values which is physically impossible. Based on this outcome, we assume that the left bound of the GSDs in mylonites is always zero.

3.2. Typical range of values describing lognormal distributions in mylonites

In nature, MSD values up to 33 has been found across different fields of science (geology, mining, ecology, etc.), although most fall within the range 1.4–3.0, and values below 1.2 are difficult to distinguish from normal (Gaussian) ones (Limpert et al., 2001). For mylonites, the data available for GSDs is rather limited, showing MSD values that range between 1.35 and 6.1 (Table 2). However, excepting the data provided in Heilbronner and Bruhn (1998), all values were estimated from apparent 2D GSDs not from actual ones. Consequently, a precise range of MSD values –or SD of log(x)– remains to be determined in dynamically recrystallized rocks.

4. A new stereological method for quantifying the actual 3D GSD in mylonites: the two-step method

The two-step method is a hybrid between a distribution-free

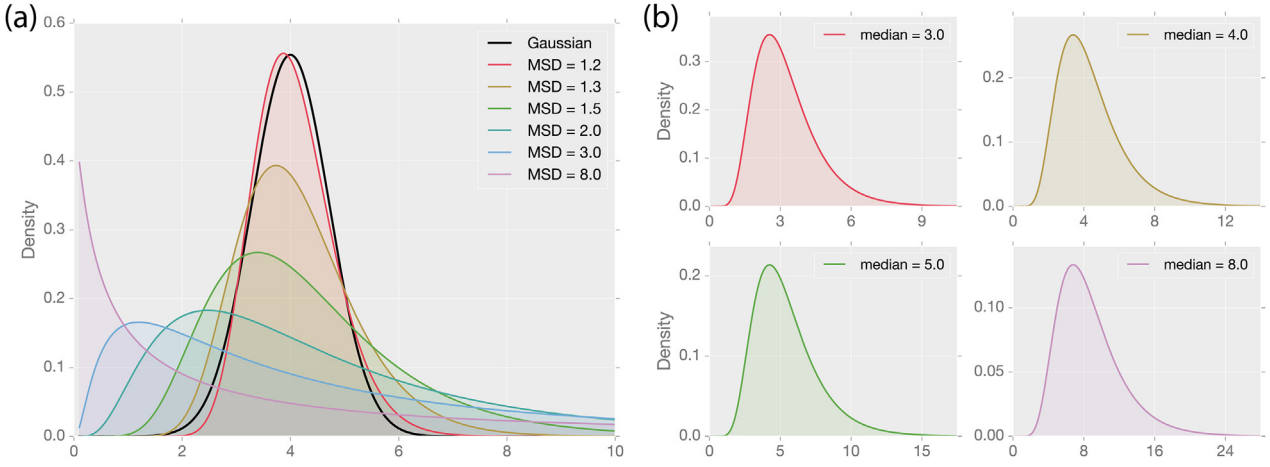

Fig. 3. Probability density functions (pdfs) of selected lognormal distributions. (a) Pdfs with different MSD or shape (μ^*) values and the same median or scale ($\mu^* = 4.0$). The MSD parameter controls the shape of the lognormal distribution. Note that although the median remains the same, the frequency peak approaches zero with increasing MSD. (b) Pdfs with different median values and the same MSD ($\sigma^* = 1.5$). A change in the median value affects the scaling in horizontal –the grain size range– and vertical directions, but the shape of the pdf remains the same. This illustrates that using a single number, the MSD value, we can define the shape of the GSD independently of its scale, which is very convenient for comparative purposes.

Table 2
Published standard deviation ranges (or values) obtained from GSDs in mylonites.

Data type	Mineral phase[a]	Standard deviation	MSD[b]	Reference
3D GSDs	Anh, Cal	1.0–1.7[c]	2.3–6.1	Heilbronner and Bruhn (1998)
2D GSDs	Qtz	0.3[d]	1.35	Shimizu (1999)
2D GSDs	Cal, Ol, Fsp	0.7–1.0[d]	2.0–2.7	Ter Heege et al. (2004) [e]

[a] Anh - Anhydrite; Cal - Calcite; Fsp - Feldspar; Ol - olivine; Qtz - Quartz.
[b] Recalculated from SD values.
[c] They provided the SD deviation using linear grain sizes.
[d] They provided a SD deviation range using logarithmic grain sizes.
[e] Data compiled from Michibayasi (1993), Newman (1994), Molli et al. (2000), and Dijkstra et al. (2002).

and a parametric (distribution-based) method. This approach has the advantage of using a well-proven distribution-free stereological method, the Saltykov method, to estimate the parameters describing the lognormal distribution using a parametric method. The first step of the method involves the measurement of the cross-sectional areas of the grains, estimating the apparent diameters via the equivalent circular diameter, and unfolding the apparent GSD using the Saltykov method. The second step, which is the parametric one, consists of fitting a lognormal probability density function to the unfolded data using the midpoints of the different classes previously estimated and a non-linear least squares algorithm (Marquardt, 1963). The detailed procedure for the two-step method is described in Appendix B.

5. Methods and materials

5.1. Representation of grain size distributions

There are different ways to represent size distributions graphically (for details see Exner, 1972; Higgins, 2006; Berger et al., 2011; Heilbronner and Barret, 2014; Lopez-Sanchez and Llana-Fúnez, 2015). In this study, our aim is to use graphs to: (i) visualize whether the distribution of grain sizes approach a log-normal distribution; (ii) compare between different distributions independently of the sample size and number of classes; and iii) optimally envisage the volume of a particular grain size fraction. For this, two types of graphs were selected (Fig. 4): (i) a frequency versus grain size plot, which is optimal in illustrating the shape of the distribution (Fig. 4a); and (ii) a volume-weighted cumulative frequency graph, which is optimal for comparative purposes (Exner, 1972) and for portraying the volume of a particular grain size fraction (Fig. 4b).

5.2. Grain size characterization

The application of any stereological method requires defining how the size of the grain profiles is measured. Most stereological methods require measuring the grain profiles individually, and therefore, we are restricted to grain-by-grain measures. In this context, a common procedure is to convert the cross-sectional areas of the individual grains into the apparent diameters via the equivalent circular diameter (e.g. Heilbronner and Bruhn, 1998; Berger et al., 2011; Lopez-Sanchez and Llana-Fúnez, 2015). This measure of the size also has the advantage compared to others that it is orientation-independent (Exner, 1972).

5.3. Testing methods

The Saltykov and the two-step methods were tested several ways to determine if they produce reliable results:

i) that different grain boundary maps belonging to the same sample, produce comparable results;
ii) that the use of different number of classes affects the reproducibility of the results;
iii) that the method produces accurate results by using synthetic samples with known probability density functions (i.e., forward or direct modelling).

The experiments (i) and (ii) are designed to test the reproducibility and precision of the estimates, but they provide no indication about their accuracy. The experiment (iii) uses several synthetic GSDs consisting of random distributions of sphere diameters that follow a specific lognormal distribution. Then, a section cutting through the aggregate of spheres is simulated considering the cut-section and the intersection probability effects (see details in

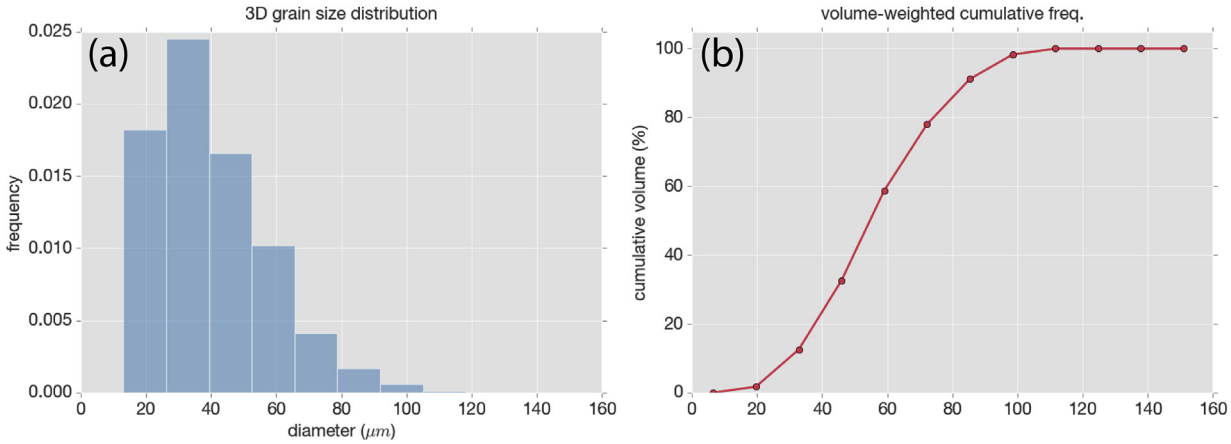

Fig. 4. Plots used in this study representing the distribution of grain sizes: (a) Frequency *vs* grain size plot in linear scale. (b) Volume-weighted cumulative frequency curve.

Appendix C). The tests were run using the GrainSizeTools script (Lopez-Sanchez, 2015). For reproducibility, the source codes and the data sets used in this study are included in the Supplementary Material.

5.4. Testing material

Sample MAL-05 comes from a coarse-grained two-mica granite affected by a Variscan crustal-scale extensional shear zone, the Vivero fault (Lopez-Sanchez, 2013; Lopez-Sanchez et al., 2015). The main constituents of the mylonite are quartz (~35%), feldspar (microcline plus plagioclase; ~60%) and muscovite plus biotite (≤5%). Mylonitic samples show quartz aggregates with a complete or quasi-complete dynamic recrystallization dominated by sub-grain rotation (Fig. 5). In contrast, feldspar shows cataclasis with syn-tectonic crystallization of very fine albite-oligoclase, K-feldspar and/or biotite grains along fractures and at the feldspar rims (Lopez-Sanchez, 2013).

For comparative purposes, several thin sections were prepared specifically for this study from the same MAL05 sample, named MAL05-A, B, C and E, respectively. A grain boundary map from each thin section was generated, measuring a total of 12,298 grain profiles (Fig. 6). The grains were segmented manually. To minimize errors in the segmentation process, we used four digital images, or mosaic of images, for each grain boundary map, a pair of cross-polarized and a pair with the gypsum plate inserted (two of them rotated 45° with respect to the others) (Fig. 6). As shown in Table 3, the different grain boundary maps show similar 1D grain size parameters, confirming that they are comparable.

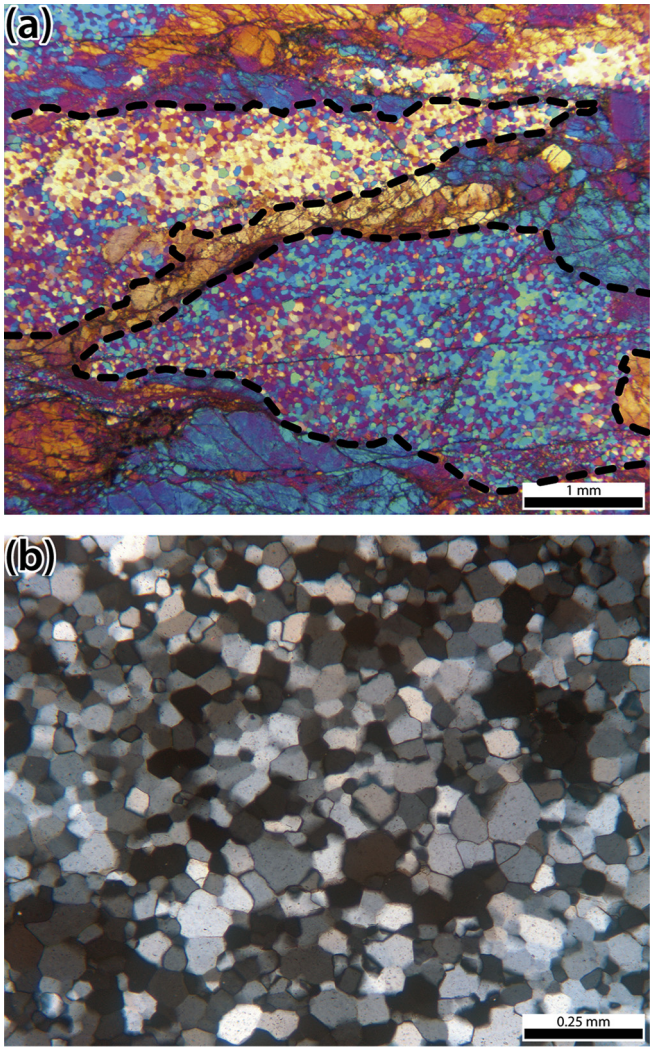

Fig. 5. Micrographs showing the quartz microstructure in sample MAL-05. (a) General view of Penedo Gordo granite mylonites under transmitted light microscopy (crossed polars, gypsum plate inserted). The image shows two original quartz grains (outlined) fully recrystallized and with a strong crystal preferred orientation. (b) Optical micrograph in crossed polars showing the typical microstructure of dynamically recrystallized quartz grains within quartz aggregates.

The strategy for testing whether the Saltykov method is applicable to our grain boundary maps due to the nearest neighbour relations imposed by the grain packing is two-fold. One is aimed at comparing the estimates between a very large data set (i.e. considering all the data; n = 12,298) and each grain boundary maps separately. The other is aimed at minimizing the nearest neighbour interactions by selecting grains randomly on a given volume of rock using a resampling technique (Fig. 6). This procedure allows to obtain apparent grain size populations free of nearest neighbour relations and compare whether the estimates are similar to those obtained using the grain boundary maps. For this, we pick grain profiles randomly at a rate of n/8 using the whole data set. This rate ensured that the resampled samples have a sample size above the minimum recommended to apply the Saltykov method (>1000 grain profiles) and that nearest neighbour relations are avoided, since the formation of grain clusters were hardly observed in the grain boundary maps (Fig. 6).

6. Results

6.1. GSD stereological estimates and the grain packing issue

Table 3 and Fig. 7a show that the 1D grain size and the volume estimates for particular grain size fractions using the Saltykov method are similar within the error considering the different grain boundary maps and the whole data set. Likewise, the same estimates in the randomly resampled samples yield similar values within the error to those estimated from the different grain boundary maps (cf. Tables 3 and 4 and Fig. 7a and b). This confirms that the grain boundary maps have sample sizes large enough to safely apply the Saltykov method, and ultimately, validate the design of experiments.

6.2. Test the Saltykov and the two-step methods using different data sets

Fig. 7a shows the results of applying the Saltykov method on different grain boundary maps belonging to the MAL-05 sample. The volume-weighted cumulative curves are similar (Fig. 7a) and the volume estimates of grain fractions, considering the fractions equal or less than 40, 60 and 80, yield comparable results with an absolute precision mostly below ±5 at a 2-sigma level of confidence (Fig. 7c).

Fig. 8 shows that the estimates for the optimal MSD and median parameters across different grain boundary maps using the two-step method yield reproducible results. Also that the error reported by the fitting procedure on each grain boundary map are reliable, i.e. within the mean calculated for all maps (Fig. 8e and f). The relative precision of the estimates at a 2-sigma level is of about ±5% for both parameters, although individual errors are at times smaller.

6.2.1. The effect of choosing a different number of classes

An additional test was conducted to constrain the effect of choosing different number of classes in the estimates of volume grain fractions. Based on previous studies, we used between 10 and

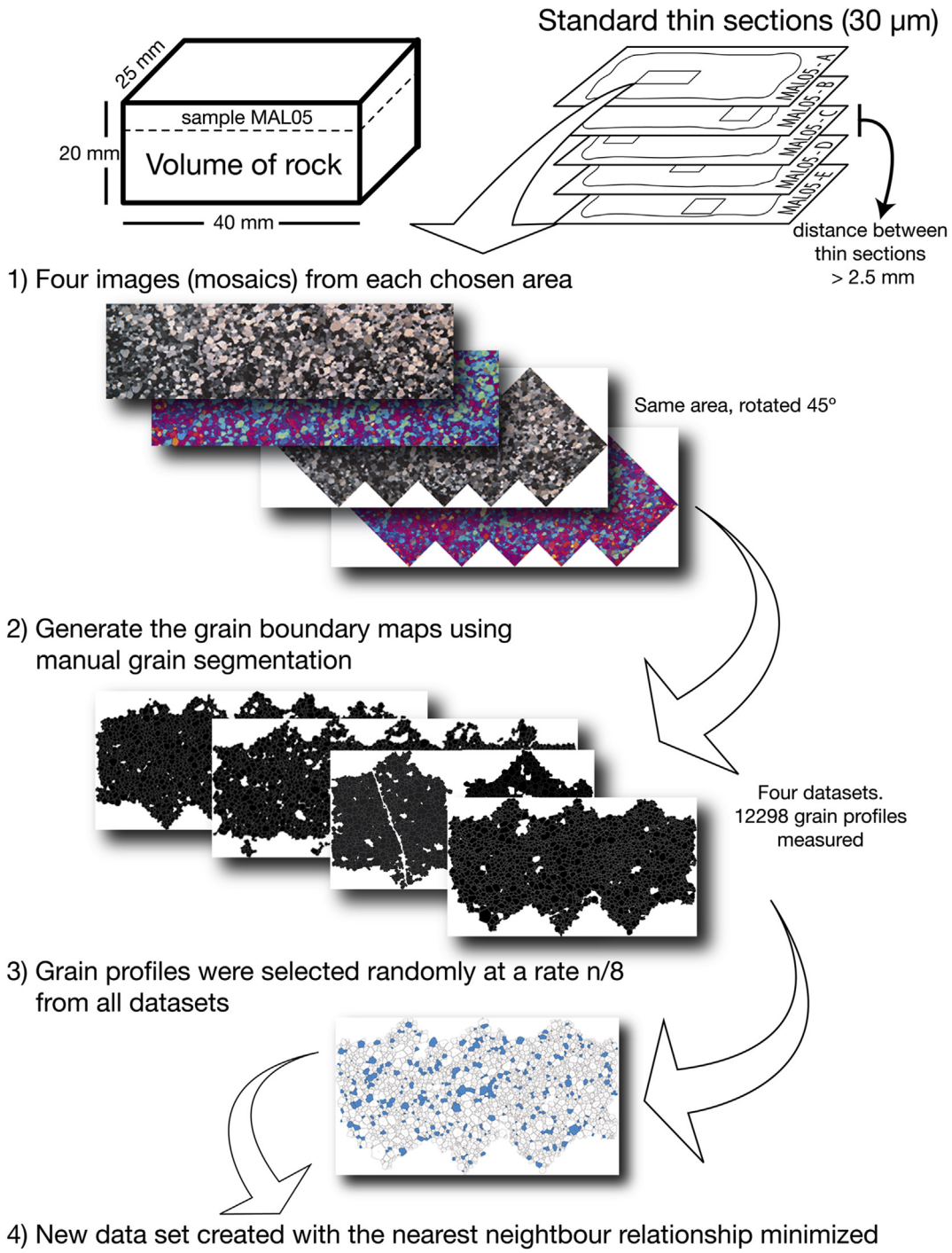

Fig. 6. Workflow to obtain the recrystallized grain boundary maps and the random resampled data sets.

20 classes.

Fig. 9a and b show that the use of a different number of classes hardly affects the appearance of the volume-weighted cumulative frequency curves using the Saltykov method. The differences obtained in the volume estimates within the interval of classes considered are below the ±5 uncertainty value. Still, it is remarkable to note that except for the extreme values of grain size, the volume estimates indicate that the larger the number of classes considered, the smaller the volume estimate for a particular grain size fraction (Fig. 9b).

Fig. 9c and d show that when the two-step method is tested against the use of different number of classes, the estimates of the median and the MSD parameters are still reproducible. Also, that the individual errors reported by the fitting procedure are reliable. The precision obtained in both parameters are in this case far below 5% (at a 2-sigma level of confidence), which is notably smaller than those obtained from different grain boundary maps (cfr. Figs. 8e, f and 9c, d). This outcome indicates that in practice the two-step method is independent of the number of classes chosen.

6.2.2. Testing the accuracy of the estimates using synthetic data sets

Fig. 10a–c show examples of volume estimates using the

Table 3
Results of 1D grain size measures in the different datasets under study.

Sample	Sample size		Mean	Median	Freq. peak	Area-weighted mean
All data[a]	**12,298**		**35.79**	**32.82**	**27.16**	**53.58**
A	2661		35.79	32.53	25.24	54.88
B	2256		36.44	33.22	26.38	53.44
C	3637		35.95	33.47	28.57	51.83
E	3744		35.24	32.08	21.63	54.44
Mean			35.86	32.83	25.46	53.65
SD (2-sigma)		±	0.86	1.10	5.02	2.34
Coeff. Var. (%)[b]		±	2.4	3.4	19.7	4.4

[a] Not considered for the statistical descriptors.
[b] Coefficient of variation considering a standard deviation at a 2-sigma level.

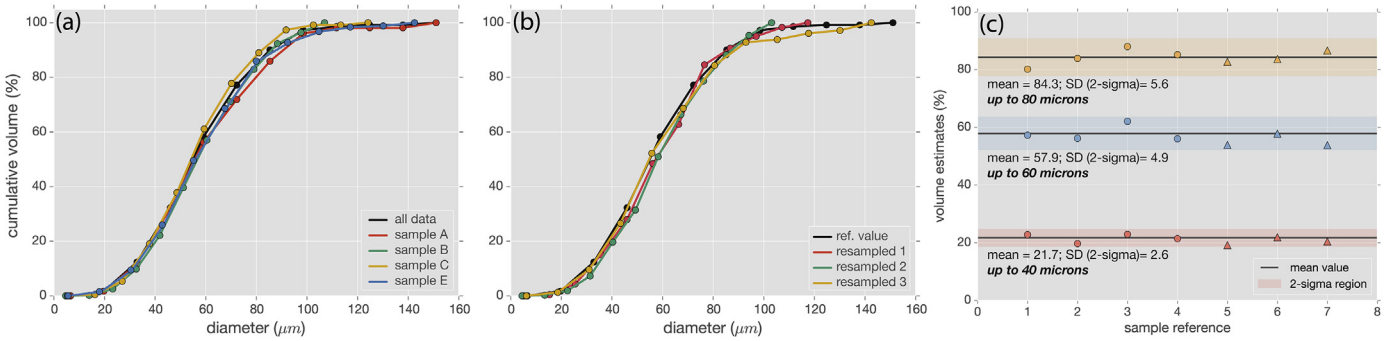

Fig. 7. Results using the Saltykov method in different data sets. (a) Volume-weighted cumulative frequency curves using different grain boundary maps from sample MAL05. (b) Volume-weighted cumulative frequency curves using the resampled data sets. Note that for reference, the curve in black is the same as in (a). (c) Volume estimates for the fractions less or equal to 40, 60, and 80 μm. Triangles denote the resampled data sets. The mean and the SD at a 2-sigma level are based on the estimates obtained from the MAL05 grain boundary maps. The estimates using the resampled data sets are within the trust area. Data used for (c) are provided as Supplementary Material.

Saltykov method in three different synthetic lognormal distributions. The results indicate that the differences between the volume estimates and the real values are smaller than ±5 for most part of the curve. As show in Fig. 10b, the cumulative frequency curves sometimes display fluctuations in the larger segment of the curves that lead to inaccuracies above the absolute ±5 uncertainty limit considered above (Fig. 10c).

Fig. 10d–f display the results using the two-step method for several synthetic lognormal distributions. Fig. 10e shows that the estimate of the optimal MSD parameter is reliable in both accuracy and precision. In contrast, Fig. 10f indicates that the estimates of the median parameter are reproducible and precise but not accurate. Specifically, the two-step method overestimated the median values showing a bias of +3.5 (+9.5%) (see Fig. 10f).

7. Discussion

7.1. The Saltykov method

Our results confirm that Saltykov method is suitable to apply in mylonitic samples as long as the sample size is large, the number of classes small and the shape of the grains not far from near-equant. The meaning of what is “large” and “small” in such context is not straightforward because both issues remain unresolved. Practical experience indicates that large samples (>1000 grains) and a range of classes between 7 and 20 are optimal to obtain reliable results. In essence, the strategy to follow involves balancing trade-offs between the measurement of a large number of grains in a reasonable time to later find an optimal number of bins by a trial and error approach.

The Saltykov method is optimal for estimating the volume percent of a particular grain size fraction and therefore for tracking changes in the volume of particular grain size fractions during deformation. An optimal approach for quantifying the uncertainty of the estimates is as described in this study. However, the process to make several representative grain boundary maps is very time-consuming and in many cases impractical. Our results show that the differences in the volume estimates considering different grain boundary maps from the same sample are typically below an absolute value of ±5 at a 2-sigma level, and far below ±5 for those involving the smallest grain fractions (Fig. 7c), which are the main target in microtectonic studies. An important finding here is that we obtain reliable estimates by assuming an uncertainty value of ±5 in the volume estimates using a single grain boundary map. However, it remains to be determined whether the uncertainty value given above is also valid using automatic or semi-automatic grain segmentation procedures (e.g. Heilbronner, 2000; Barraud, 2006) instead of manual outlining.

An important finding, shown in Fig. 9a and b, is that the use of a different number of classes is not a major concern for comparative purposes across studies. Thus, the differences in the estimates using the same data set and considering 10 to 20 classes were better

Table 4
Results of 1D grain size measures in the resampled samples.

Sample		Mean	Median	Freq. peak	Area-weighted mean
r1		36.30	33.45	27.11	53.90
r2		35.74	32.85	28.72	54.23
r3		35.40	32.54	25.75	53.42
Mean		35.81	32.95	27.19	53.85
SD (2-sigma)	±	0.74	0.76	2.43	0.67
Coeff. Var. (%)[a]	±	2.1	2.3	8.9	1.2

[a] Coefficient of variation considering a standard deviation at a 2-sigma level.

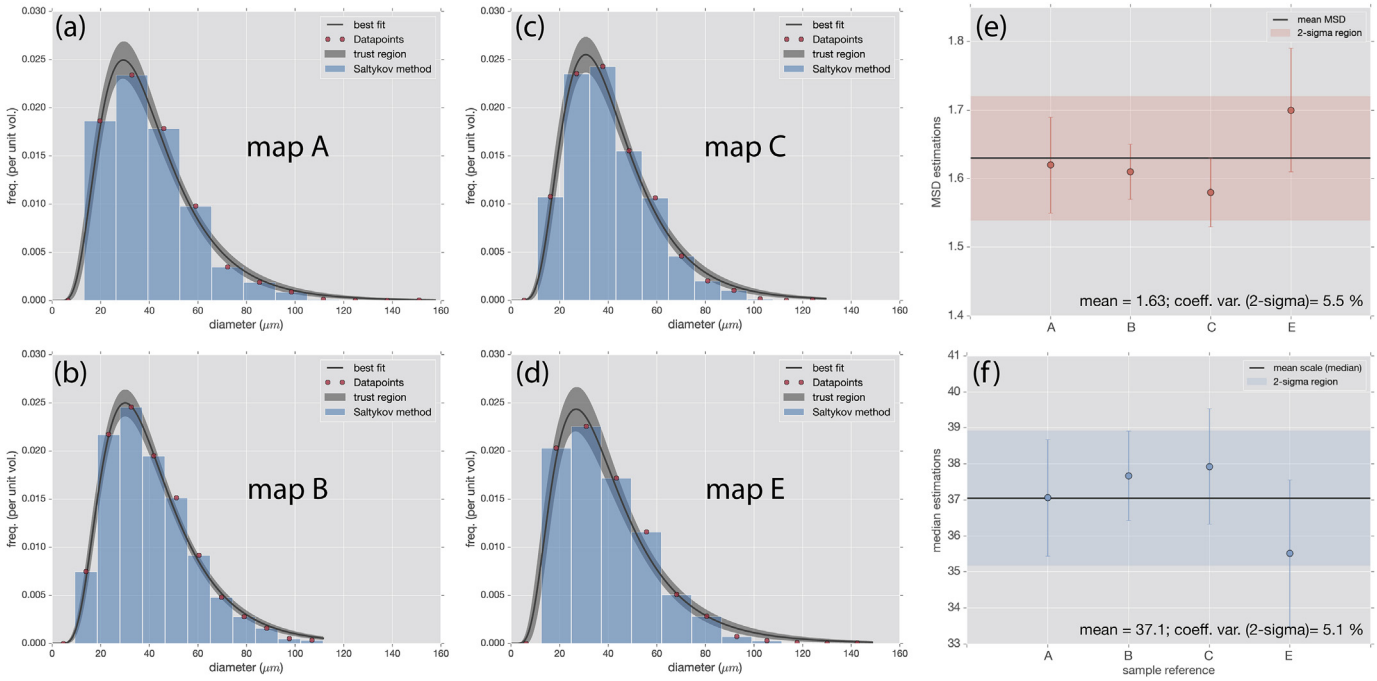

Fig. 8. Estimates of the lognormal optimal parameters using the two-step method over different grain boundary maps from sample MAL05. We used 12 classes for all estimates. (a–d) Fitted lognormal distributions (e) Optimal MSD estimates. The error bars display the uncertainty value reported by the fitting procedure. The mean (black line) and the SD (2-sigma level) region were estimated considering all data sets. (f) The same as (e) but for the median parameter. Data used to make the figures (e) and (f) are provided in the Supplementary Material.

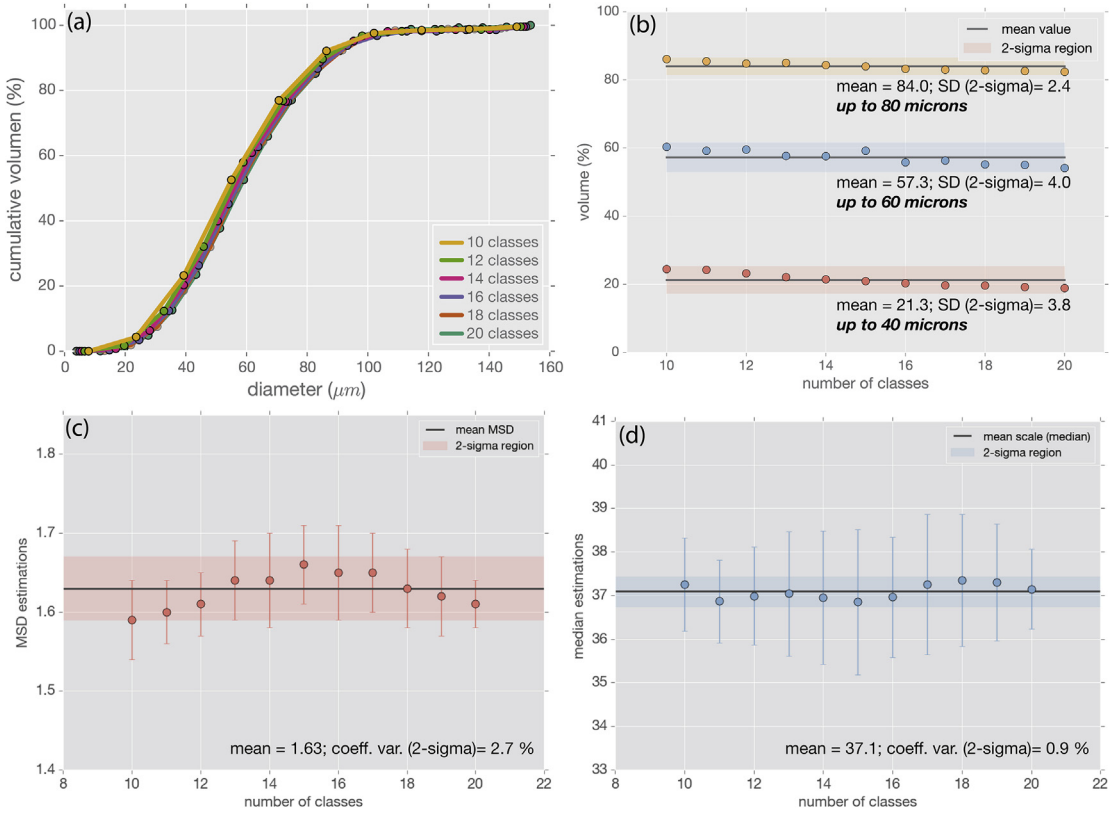

Fig. 9. Different estimates using different number of classes on the same data set. (a) Volume-weighted cumulative frequency curves using the Saltykov method. (b) Volume estimates for the fractions less than or equal to 40, 60, and 80 μm. Note a slightly inverse trend between the volume estimated and the number of classes considered. (c) Optimal MSD estimates using the two-step method with individual errors and the mean and SD (2-sigma) considering all data. (d) The same as (c) but for median estimates. Data used to make (b), (c), and (d) are provided in the Supplementary Material.

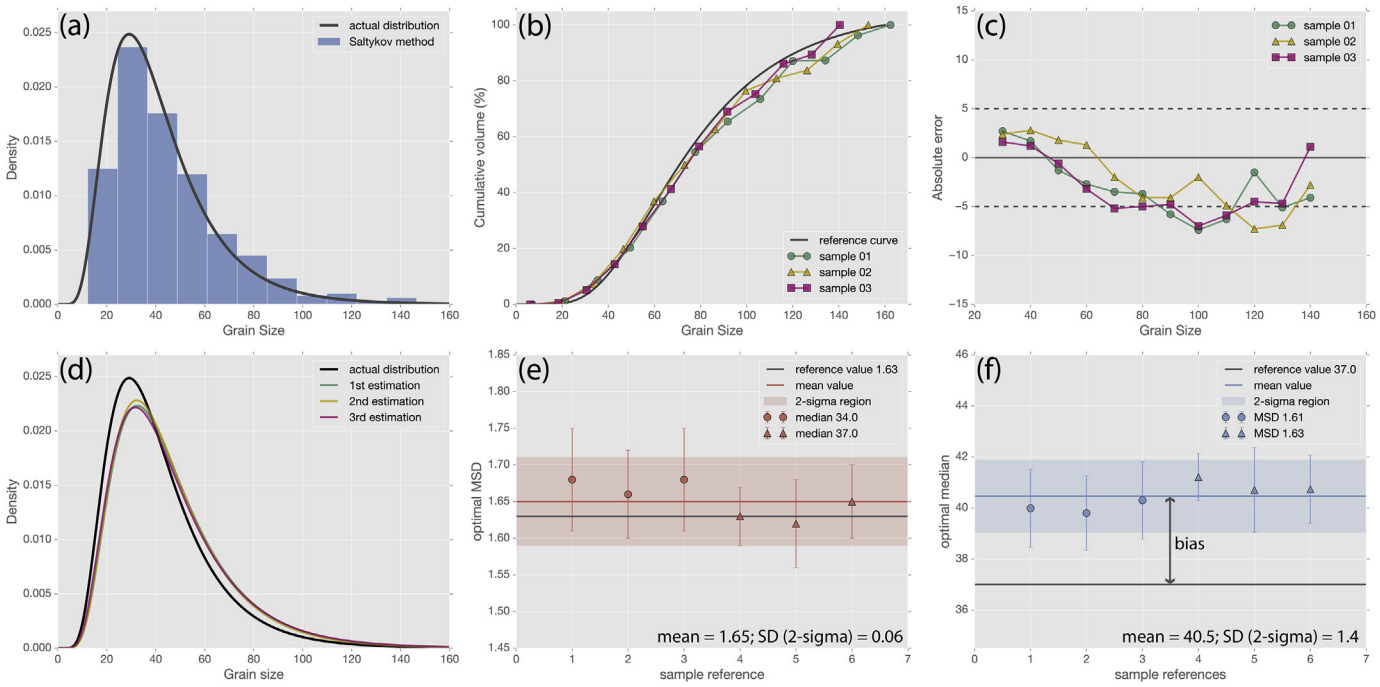

Fig. 10. Examples of estimates obtained using synthetic data sets of GSDs. Each synthetic population have 3000 spherical grains. (a) An example of a synthetic lognormal population and the unfolded population using the Saltykov method. (b) Volume-weighted cumulative frequency curves in three different data sets using the Saltykov method with MSD = 1.61 and median = 37. The reference curve (in black) has a hypothetical grain size range from 0 to 160. (c) Absolute errors with respect to reference curve for the three estimated curves. The method yields accurate (≤5) volume estimates for the smallest grain fractions (~up to 80 μm in the present case). In contrast, the largest grain fractions suffer from fluctuations in the accuracy. (d) Probability density curves estimated by the two-step method from three different thin sections belonging to the same (i.e. the actual) population of grains. The actual distribution is the same shown in (a). (e) Optimal MSD estimates using synthetic populations with a fixed MSD value (1.63) and two different median values. The mean and SD (2-sigma) of all data and the reference value of MSD are plotted. (f) Same as (e) but for median estimates. The synthetic populations have the same median value (37) but different MSD values. The bias is indicated. Data used to make (b), (c), (e) and (f) are provided in the Supplementary Material.

than the absolute ±5 uncertainty value. Therefore, in practice the method is independent of the number of classes chosen as long as the use of an excessive number of classes in the Saltykov method is avoided.

A note of caution with this general uncertainty value for volume estimates needs to be raised because the volume-weighted cumulative frequency curves sometimes display fluctuations that lead to inaccuracies greater than the absolute ±5 uncertainty limit (Fig. 10b and c). This situation occurs mostly for the larger grain size fractions (Fig. 10c). However, these fluctuations are easy to visualize in the volume-weighted cumulative frequency curves since they possess a very distinctive sigmoidal shape. It is therefore crucial to always inspect the volume-weighted cumulative frequency curves when estimating the volume of particular grain fraction.

7.2. The two-step method

Our results show that the two-step method is suitable for describing quantitatively the shape of the actual GSD from a single section. A significant finding is that the uncertainty value returned by the fitting procedure is reliable by itself, and therefore is unnecessary to make several grain boundary maps to obtain an uncertainty value in the estimates. The advantages of using a method in two steps instead of applying directly a parametric method are twofold. The first step allows the user to test whether the assumption of lognormality is valid and the parametric method applicable. Second, the use of the Saltykov method in the initial step helps to mitigate the introduction of errors by smoothing the distribution of data using the histogram. This approach allows estimating a plausible approximation of the distribution of grain sizes to later fit a lognormal probability density function.

On the other hand, the method is limited to samples with complete dynamic recrystallization (i.e. unimodal lognormal-like distributions), or when the non-recrystallized grains can be discarded from the whole population based on shape descriptors. Another current limitation of the method is that the estimate of the median although precise is inaccurate (i.e. the true value is slightly smaller and outside the precision reported). We suspect that the bias observed in this study is systematic and it would be possible in the future to estimate a correction factor using a comprehensive set of grain size data.

The two-step method also allows estimating a volume-weighted cumulative frequency curves with trust regions. However, the shape of these curves is very sensitive to changes in the range of the grain size, producing significant changes in the segment of the curves with the larger grain size fractions (Fig. 11). As shown in Fig. 8a–d, variations in grain size ranges are expected even when considering different grain boundary maps from the same sample. As deduced from Fig. 7 and the data provided in the Supplementary Material, the use of the Saltykov method mitigates this effect, and it is therefore preferred for estimating the volume of grain size fractions.

In summary, the two-step method provides a practical quantitative description of the actual 3D GSDs shape in mylonites that goes far beyond to what has been done so far. The strengths of the method can be summarized as follows:

i) it allows estimation of the optimal parameters describing the actual 3D GSD from a single section, obtaining reproducible results;

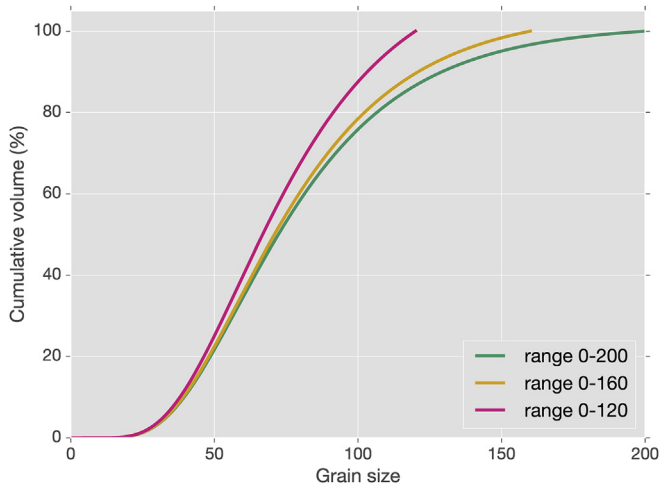

Fig. 11. Comparison between three volume-weighted cumulative curves belonging to the same lognormal population (MSD = 1.61 and median = 37) but considering different ranges of grain size.

ii) in practice the method is independent of the chosen number of classes;
iii) the fitting procedure provides by itself reliable error estimates;
iv) the estimate of the MSD (i.e. the shape of the GSD) is accurate and precise, with a typical uncertainty equal or better than ±5% at a 2-sigma level;

The two-step method will help scientists to define a reliable range of MSD values in different rock-forming minerals, improving the understanding of the rheological properties of crystalline aggregates and the constraints on dynamic recrystallization models. In fact, the application of the two-step method in this study provides the first typical MSD value (1.63 ± 0.04 for a median ~ 37.0) in recrystallized quartz mylonites. This value disagrees with the range of values reported by Ter Heege et al. (2004) for different recrystallized rock-forming minerals once recalculated to MSD (2.01–2.71), as well as with the value considered by Shimizu (1999) in recrystallized quartz (1.35). We therefore recommend that 2D GSDs not be used for estimating these values, as has been previously done.

Finally, with the aim of facilitating the use of the Saltykov and the two-step methods, we put both methods in a free and open-source script that can be downloaded from different permanent sites (see http://marcoalopez.github.io/GrainSizeTools/).

8. Conclusions

1) The Saltykov and the two-step method are suitable to characterize GSDs in crystalline aggregates with random grain packing, such as mylonites, as long as sample size is large enough, the number of classes small, and the shape of the grains not far from near-equant. The minimum number of grains needed for applying the Saltykov method and the best number of classes remains unresolved, but practical experience indicates more than 1000 grains and less than 20 classes. The optimal number of classes has to be set by a trial and error approach.
2) The Saltykov method is suitable to estimate the volume of a particular grain fraction with absolute errors below ±5. In practice, this error is independent of the number of classes chosen.
3) The two-step method is suitable for describing quantitatively the shape of the actual GSD from a single section, and providing a reliable uncertainty value. This estimate is independent of the number of classes. The precision obtained is typically better than 5% at a 2-sigma level. The MSD (i.e. the shape of the GSD) estimates are accurate, while the median estimates are slightly overestimated.
4) Using the two-step method, we estimate a MSD value of 1.63 ± 0.04 in recrystallized quartz from a natural quartz mylonite. This value disagrees with previous estimates that used apparent 2D GSDs.

Acknowledgements

We thank Michael Stipp, Alfons Berger, and the editor William Dunne for improving the content and the focus in the manuscript. This work was supported by the Spanish Ministry of Economy and Competitiveness (MINECO) excellence research [grant number CGL2014-53388-P].

Appendices

Appendix A. The (Scheil-Schwartz)-Saltykov method

The procedure is based on the Wicksell (1925) analytical solution of the corpuscle problem, and involves an estimate of the probability distribution of spheres for a particular grain size interval. Based on previous works by Scheil (1931) and Schwartz (1934), Saltykov (1949) proposed a general "successive subtraction algorithm" to unfold the different classes or grain size intervals of the apparent grain-size distribution into the actual one using the expression:

$$P(r_1 < r < r_2) = {}^{1}/_{R}\sqrt{R^2 - r_1^2} - \sqrt{R^2 - r_2^2} \quad \text{(A1)}$$

where R is the radius of the sphere (i.e. the grain), r_1 and r_2 the lower and upper limits of the interval of apparent sizes defined, and P the probability to cut sections within the interval defined. Differences between different implementations lie in choosing where to place R with respect to the different defined classes. Most authors placed R at the upper limit of each class (e.g. Saltykov, 1967; Sahagian and Proussevitch, 1998), others at the midpoint of the classes (e.g. Higgins, 2000) or even at the lower limit. Since true particle sizes are distributed throughout the interval of each class, we set the value of R at the centre of the classes. Therefore, the algorithm in the GrainSizeTools script (v.1.0 or higher) takes the midpoints of the classes and then estimate the number of theoretical apparent sections that fall within each class interval to subtract them iteratively.

Appendix B. Description of the procedure to apply the two-step method

The first step requires applying the Saltykov method to unfold distribution of 2D grain profile sizes into the actual 3D distribution. This step allows us to test whether the assumption of log-normality is valid.

Once this step is completed, the method fits a lognormal function with base e via regression using the midpoints of the classes. For this step, the method uses a well-proved non-linear least-square routine, named the Levenberg–Marquardt algorithm (Marquardt, 1963) calling the Python *scipy.optimize* package (Oliphant, 2007). This routine minimizes the sum of squares of a set of equations and offers the best fit from any kind of function. In this

case, the function describes a lognormal distribution. The script returns the optimal MSD and median values as well as the variance found during the fitting procedure, which allows estimation of the standard deviations and definition of a trust region. The pseudocode of the procedure as put in the GrainSizeTools script is:

1. Estimate the histogram of the apparent 2D grain-size distribution. The left edge is set to zero and the number of classes is set to ten by default, although the user can define any number of classes.
2. A Saltykov-type successive subtraction algorithm is applied to unfold the distribution of apparent grain sizes into the actual GSD. If frequency negative values appear, they are replaced by zero. Then, the histogram is normalized so that the integral over the full range is equal to one (i.e. the frequencies are first normalized to one and then divided by the bin size).
3. At this point, if the user specified application of the classic Saltykov method, the script returns two graphs: i) the frequency vs grain size and ii) the volume-weighted cumulative grain size curve. In addition, the user can set a limit of grain size to estimate the percentage of volume of a particular grain size fraction. As an example if the user set this limit to 40 μm, the script returns the percentage of volume corresponding to all existing grain size fractions below or equal to that value. To calculate this percentage, the script uses an approximation by triangulation using the nearby midpoints.
4. If the user specified application of the two-step method, then the procedure starts to find the optimal MSD and median parameters using the Levenberg–Marquardt algorithm. The algorithm only converges to the global minimum if the initial guesses for both parameters are already somewhat close to the final solution. Based on the results obtained in this study, the algorithm uses as default values 1.2 (MSD) and 25.0 (median). However, sometimes it is necessary to set different guess values to find a correct solution. To support application of a guess, the script allows the user to set alternative initial guess values.
5. Once the best fit is obtained, the script returns: i) the optimal MSD and median values; ii) the uncertainty of the fitting at a 3-sigma level; and iii) a frequency vs diameter graph showing the lognormal distribution of grain sizes, the midpoints of the classes, and the trust region.

Appendix C. A stochastic model to simulate apparent grain size distributions from lognormal grain size distributions

The procedure to generate synthetic 2D sections from lognormal populations of spheres assumes that:

- Particles (grains) are spherical
- The particle population is distributed homogeneously in space.
- No nearest neighbour relationship exists between grains. We assume that as long as the sample size chosen is large enough (>1000), the nearest neighbour relationship between grains can be ignored.
- The intersection probability and the cut-section effects apply.

The pseudocode of the procedure implemented is:

1) A lognormal distribution of diameters with a defined median and MSD values is generated (n = 3000). For this procedure, we used the *lognorm.rvs* routine in the Python *scipy.stats* v. 0.16 package (Oliphant, 2007)
2) The intersection probability effect is simulated using the equation (Fullman, 1953; DeHoff and Rhines, 1961):

$$N_A = d_v\, N_V \tag{C1}$$

where N_A is the number of particle profiles per unit area in a plane section, d_v is the average length of the particle (in the present case, the diameter), and N_V is the number of particles per unit volume of the material. The procedure discretizes the sphere (grain) size range into classes and apply this equation using the midpoints of the classes as a reference for d_v. N_V is estimated using the number of particles within each class per unit volume, taking the volume of the entire population as a unit volume. By assuming that the unit volume is a cube and that the plane section a square, we can estimate the number of particles in the simulated plane section (N_A). Finally, the procedure removes randomly the excess of spheres (grains) from each class so that the number of particles to be represented in the simulated section plane coincides with the theoretical values estimated by Eq. (C1).

3) Finally, all the spheres are sectioned randomly to apply the cut-section effect. The procedure to do this is explained in Appendix B of Lopez-Sanchez and Llana-Fúnez (2015).

Appendix. Supplementary data

Supplementary data related to this article can be found at http://dx.doi.org/10.1016/j.jsg.2016.10.008.

References

Barraud, J., 2006. The use of watershed segmentation and GIS software for textural analysis of thin sections. J. Volcanol. Geotherm. Res. 154, 17–33. http://dx.doi.org/10.1016/j.jvolgeores.2005.09.017.

Berger, A., Herwegh, M., Schwarz, J.O., Putlitz, B., 2011. Quantitative analysis of crystal/grain sizes and their distributions in 2D and 3D. J. Struct. Geol. 33, 1751–1763. http://dx.doi.org/10.1016/j.jsg.2011.07.002.

Casey, M., Kunze, K., Olgaard, D.L., 1998. Texture of Solnhofen limestone deformed to high strains in torsion. J. Struct. Geol. 20, 255–267. http://dx.doi.org/10.1016/S0191-8141(97)00058-8.

Chiu, S.N., Stoyan, D., Kendall, W.S., Mecke, J., 2013. Stochastic Geometry and its Applications, third ed. John Wiley & Sons.

Cruz-Orive, L.M., 1983. Distribution-free estimation of sphere size distributions from slabs showing overprojection and truncation, with a review of previous methods. J. Microsc. 131, 265–290. http://dx.doi.org/10.1111/j.1365-2818.1983.tb04255.x.

De Bresser, J.H.P., Peach, C.J., Reijs, J.P., Spiers, C.J., 1998. On dynamic recrystallization during solid state flow: effects of stress and temperature. Geophys. Res. Lett. 25, 3457–3460. http://dx.doi.org/10.1029/98GL02690.

De Bresser, J.H.P., Ter Heege, J.H., Spiers, C.J., 2001. Grain size reduction by dynamic recrystallization: can it result in major rheological weakening? Int. J. Earth Sci. 90, 28–45. http://dx.doi.org/10.1007/s005310000149.

DeHoff, R., Rhines, F., 1961. Determination of number of particles per unit volume from measurements made on random plane sections: the general cylinder and the ellipsoid. Trans. Met. Soc. AIME 221, 975–982.

Derby, B., Ashby, M.F., 1987. On dynamic recrystallization. Scr. Metall. 21, 879–884. http://dx.doi.org/10.1016/0036-9748(87)90341-3.

Dijkstra, A.H., Drury, M.R., Frijhoff, R.M., 2002. Microstructures and lattice fabrics in the Hilti mantle section (Oman Ophiolite): evidence for shear localization and melt weakening in the crust–mantle transition zone? J. Geophys. Res. http://dx.doi.org/10.1029/2001JB000458.

Exner, H.E., 1972. Analysis of grain- and particle-size distributions in metallic materials. Int. Metall. Rev. 17, 25–42. http://dx.doi.org/10.1179/imtlr.1972.17.1.25.

Fullman, R.L., 1953. Measurement of particle size in opaque bodies. Trans. Met. Soc. AIME 197, 447–452.

Heilbronner, R., 2000. Automatic grain boundary detection and grain size analysis using polarization micrographs or orientation images. J. Struct. Geol. 22, 969–981. http://dx.doi.org/10.1016/S0191-8141(00)00014-6.

Heilbronner, R., Barret, S., 2014. Image Analysis in Earth Sciences. Springer-Verlag Berlin Heidelberg. http://dx.doi.org/10.1007/978-3-642-10343-8.

Heilbronner, R., Bruhn, D., 1998. The influence of three-dimensional grain size distributions on the rheology of polyphase rocks. J. Struct. Geol. 20, 695–705. http://dx.doi.org/10.1016/S0191-8141(98)00010-8.

Herwegh, M., De Bresser, J.H.P., Ter Heege, J.H., 2005. Combining natural microstructures with composite flow laws: an improved approach for the extrapolation of lab data to nature. J. Struct. Geol. 27, 503–521. http://dx.doi.org/10.1016/j.jsg.2004.10.010.

Higgins, M.D., 2006. Quantitative Textural Measurements in Igneous and Metamorphic Petrology. Cambridge University Press.

Higgins, M.D., 2000. Measurement of crystal size distributions. Am. Mineral. 85, 1105–1116. http://dx.doi.org/10.2138/am-2000-8-901.
Holmes, A., 1927. Petrographic Methods and Calculations. Thomas Murby & Co, London.
Humphreys, F.J., Hatherly, M., 2004. Recrystallization and Related Annealing Phenomena, second ed. Elsevier Ltd.
Limpert, E., Stahel, W.A., Abbt, M., 2001. Log-normal distributions across the sciences: keys and clues. Bioscience 51 (341). http://dx.doi.org/10.1641/0006-3568(2001)051[0341:LNDATS]2.0.CO;2.
Linckens, J., Bruijn, R., Skemer, P., 2014. Dynamic recrystallization and phase mixing in experimentally deformed peridotite. Earth Planet. Sci. Lett. 388, 134–142. http://dx.doi.org/10.1016/j.epsl.2013.11.037.
Lopez-Sanchez, M.A., 2015. GrainSizeTools Script. figshare. http://dx.doi.org/10.6084/m9.figshare.1383130.
Lopez-Sanchez, M.A., 2013. Análisis tectónico de la Falla de Vivero (Galicia, NO de España). Ph.D. thesis. Universidad de Oviedo. http://hdl.handle.net/10651/20282.
Lopez-Sanchez, M.A., Llana-Fúnez, S., 2015. An evaluation of different measures of dynamically recrystallized grain size for paleopiezometry or paleowattometry studies. Solid Earth 6, 475–495. http://dx.doi.org/10.5194/se-6-475-2015.
Lopez-Sanchez, M.A., Marcos, A., Martínez, F.J., Iriondo, A., Llana-Fúnez, S., 2015. Setting new constrains on the age of crustal-scale extensional shear zone (Vivero fault): implications for the evolution of Variscan orogeny in the Iberian massif. Int. J. Earth Sci. 104, 927–962. http://dx.doi.org/10.1007/s00531-014-1119-1.
Mancktelow, N.S., Pennacchioni, G., 2004. The influence of grain boundary fluids on the microstructure of quartz-feldspar mylonites. J. Struct. Geol. 26, 47–69. http://dx.doi.org/10.1016/S0191-8141(03)00081-6.
Marquardt, D.W., 1963. An algorithm for least-squares estimation of nonlinear parameters. J. Soc. Ind. Appl. Math. 11, 431–441. http://dx.doi.org/10.1137/0111030.
McDonald, S.A., Reischig, P., Holzner, C., Lauridsen, E.M., Withers, P.J., Merkle, A.P., Feser, M., 2015. Non-destructive mapping of grain orientations in 3D by laboratory X-ray microscopy. Sci. Rep. 5, 14665. http://dx.doi.org/10.1038/srep14665.
Michibayashi, K., 1993. Syntectonic development of a strain-independent steady-state grain size during mylonitization. Tectonophysics 222, 151–164. http://dx.doi.org/10.1016/0040-1951(93)90046-M.
Michibayashi, K., Masuda, T., 1993. Shearing during progressive retrogression in granitoids: abrupt grain size reduction of quartz at the plastic-brittle transition for feldspar. J. Struct. Geol. http://dx.doi.org/10.1016/0191-8141(93)90003-S.
Molli, G., Conti, P., Giorgetti, G., Meccheri, M., Oesterling, N., 2000. Microfabric study on the deformational and thermal history of the Alpi Apuane marbles (Carrara marbles). Italy. J. Struct. Geol. 22, 1809–1825. http://dx.doi.org/10.1016/S0191-8141(00)00086-9.
Newman, J., 1994. The influence of grain size and grain size distribution on methods for estimating paleostresses from twinning in carbonates. J. Struct. Geol. 16, 1589–1601. http://dx.doi.org/10.1016/0191-8141(94)90129-5.
Oliphant, T.E., 2007. Python Sci. Comput. Comput. Sci. Eng 9, 10–20. http://dx.doi.org/10.1109/MCSE.2007.58.
Ranalli, G., 1984. Grain size distribution and flow stress in tectonites. J. Struct. Geol. 6, 443–447. http://dx.doi.org/10.1016/0191-8141(84)90046-4.
Rowenhorst, D.J., Lewis, A.C., Spanos, G., 2010. Three-dimensional analysis of grain topology and interface curvature in a β-titanium alloy. Acta Mater 58, 5511–5519. http://dx.doi.org/10.1016/j.actamat.2010.06.030.
Sahagian, D.L., Proussevitch, A.A., 1998. 3D particle size distributions from 2D observations: stereology for natural applications. J. Volcanol. Geotherm. Res. 84, 173–196. http://dx.doi.org/10.1029/95JB02500.
Saltykov, S.A., 1967. The determination of the size distribution of particles in an opaque material from a measurment of the size distribution of their sections. In: Elias, H. (Ed.), Proceedings of the Second International Congress for STEREOLOGY. Springer Berlin Heidelberg, Berlin, Heidelberg, pp. 163–173. http://dx.doi.org/10.1007/978-3-642-88260-9_31.
Saltykov, S.A., 1949. Calculation of the Distribution Curves for the Size of Dispersed Grains, vol. 1317. Plant Lab.
Scheil, E., 1931. Die Berechnung der Anzahl und Großenverteilung kugelförmiger Kristalle in undurchsichtigen Körpern mit Hilfe der durch einen ebenen Schnitt erhaltenen Schnittkreise. Z. Anorg. Allg. Chem. 201, 259–264. http://dx.doi.org/10.1002/zaac.19312010123.
Schwartz, H.A., 1934. The metallographic determination of the size distribution of temper carbon nodules. Met. Alloy 5, 139.
Shimizu, I., 2008. Theories and applicability of grain size piezometers: the role of dynamic recrystallization mechanisms. J. Struct. Geol. 30, 899–917. http://dx.doi.org/10.1016/j.jsg.2008.03.004.
Shimizu, I., 1999. A stochastic model of grain size distribution during dynamic recrystallization. Philos. Mag. A 79, 1217–1231. http://dx.doi.org/10.1080/014186199252309.
Shimizu, I., 1998. Lognormality in crystal size distribution in dynamic recrystallization. Forma 13, 1–11.
Slotemaker, A.K., 2006. Dynamic Recrystallization and Grain Growth in Olivine Rocks. Ph.D. thesis. Universiteit Utrecht.
Snoke, A.W., Tullis, J., Todd, V.R., 1999. Fault-related Rocks: a Photographic Atlas. Princeton University Press, Princeton, NJ.
Stipp, M., Kunze, K., 2008. Dynamic recrystallization near the brittle-plastic transition in naturally and experimentally deformed quartz aggregates. Tectonophysics 448, 77–97. http://dx.doi.org/10.1016/j.tecto.2007.11.041.
Ter Heege, J.H., De Bresser, J.H.P., Spiers, C.J., 2004. Composite flow laws for crystalline materials with log-normally distributed grain size: theory and application to olivine. J. Struct. Geol. 26, 1693–1705. http://dx.doi.org/10.1016/j.jsg.2004.01.008.
Ter Heege, J.H., De Bresser, J.H.P., Spiers, C.J., 2002. The influence of dynamic recrystallization on the grain size distribution and rheological behaviour of Carrara marble deformed in axial compression. Geol. Soc. London Spec. Publ. http://dx.doi.org/10.1144/GSL.SP.2001.200.01.19.
Underwood, E.E., 1970. Quantitative Stereology. Addison-Wesley Educational Publishers Inc.
Wicksell, S.D., 1925. The corpuscle problem: a mathematical study of a biometric problem. Biometrika 17, 84–99. http://dx.doi.org/10.2307/2332027.
Yuan, P.-T., 1933. On the logarithmic frequency distribution and the semi-logarithmic correlation surface. Ann. Math. Stat. 4, 30–74.